

Design of mobile stage location system based on two-dimensional laser radar^①

WANG Bo(王 波)^{②*}, ZHU Ping^{*}, ZHENG Qingsong^{*}, YANG Jiaqi^{**}

(* Yiwu Industrial and Commercial College, Yiwu 322000, P. R. China)

(** Department of Automation, Zhejiang University of Technology, Zhejiang Provincial United Key Laboratory of Embedded Systems, Hangzhou 310032, P. R. China)

Abstract

This paper addresses the design problem of an embedded mobile stage location system based on a two-dimensional laser radar. The mobile stage is a piece of important performance equipment in art performances, and the positioning problem is one of the key issues in the control of the mobile stage. Both hardware and software are developed for the mobile stage. The hardware of the location system consists of a laser radar, an embedded control board, a wireless router, and a motion control unit. The software of the location system includes embedded software and human-machine interface (HMI), and they are designed to achieve the functions of real-time positioning and monitoring. First, a novel landmark identification method is presented based on the landmark reflection intensities and shapes. Then, the initial pose of the mobile stage is calculated by using the triangle matching algorithm and the least squares method. A distributed fusion Kalman filtering algorithm is applied to fuse landmark information and odometer information to achieve real-time positioning of the mobile stage. The designed system has been implemented in a practical mobile stage, and the results demonstrate that the location system can achieve a high positioning precision in both the stationary and moving scenarios.

Key words: mobile stage positioning, laser radar, Kalman filter, distributed fusion

0 Introduction

In recent years, with the improvement of people's living standards, the demand for art activities has grown rapidly, and the importance of cultural facilities construction has become increasingly prominent. This places higher demands on the technology development of theatres and other art performance venues. More and more high-tech devices have been used in art performance venues, which gradually enrich the appreciation of the art performance. The mobile stage is a piece of important performance equipment, which can switch the scenery quickly and brings great convenience to the art performance. Besides, it can enhance the performance of the art activities and reduce the restrictions on art creation in a fixed stage. At present, the mobile stages used in the theaters are orbital or wheeled. The orbital mobile stage is implemented on the track inside the main stage and is guided by a chain or a rack. The

orbital mobile stage has accurate positioning; nevertheless, it suffers from flexibility deficiency and cannot adapt to the flexible forms of the art performances. The wheeled mobile stage drives the stage by moving the wheels and calculates the stage position according to the data of the driving wheels or the passive wheel encoders. Since there is no orbit restriction, it is more flexible and convenient to use, and has a better application prospect. However, due to wheel slippage and cumulative positioning errors, existing wheeled mobile stages cannot achieve long-term movements, and some challenging problems remain to be solved.

The positioning problem is one of the key issues in the control of the mobile stage. Due to the contradiction between the positioning precision and the movement flexibility of the mobile stage, it is necessary to accurately locate the mobile stage without limiting its movement path. The existing positioning methods include visual positioning method^[1-5], ultra-wideband (UWB) positioning method^[6-9], laser positioning method^[10-17], etc.

① Supported by the Philosophy and Social Sciences Planning Project of Zhejiang Province (No. 23NDJC374YB) and the Major Humanities and Social Sciences Research Projects in Zhejiang Higher Education Institutions (No. 2024QN067).

② To whom correspondence should be addressed. E-mail: wangbo@ywicc.edu.cn.

Received on Feb. 29, 2024

The visual positioning method depends on a clear line of sight between the source and the sensor, and can only be used in a laboratory environment. This method requires substantial computational resources and is sensitive to lighting conditions and occlusions, which limits its practical application. Ultra-wideband positioning methods can achieve a positioning precision of up to 0.1 m and are less affected by environmental factors compared with visual methods. However, they remain sensitive to occlusions and do not provide posture information of the mobile stage, restricting their practical applications. Laser positioning methods use laser radar to scan the surrounding environment and match the map to obtain the pose of the stage. These methods are less influenced by lighting conditions and are more suited for practical mobile stage applications. Laser positioning can be categorized into environment-based^[18] and landmark-based^[19-20]. The environment-based positioning method relies on the contour of the environment to determine the stage's position. This method is commonly applied in sweeping robots. However, in practical mobile stage applications, the stage area is very large, and there are no significant environmental characteristics around the stage. As a result, the environment-based positioning method cannot obtain sufficient environmental contour features, making it impractical for mobile stage positioning. On the other hand, the landmark-based positioning method involves placing passive reflective markers around the stage. This method greatly expands the laser detection distance and achieves higher positioning accuracy. It is more robust in environments with unclear environmental contours, making it more suitable for mobile stage applications. The landmark-based method is particularly advantageous due to its high precision and reliability in dynamic and variable lighting conditions typically encountered in performance venues.

This paper presents a landmark-based mobile stage laser positioning system that integrates both hardware and software components. The hardware includes a laser radar, an embedded control board, a wireless router, and a motion control unit, while the software consists of embedded software and a human-machine interface (HMI) for real-time positioning and monitoring of the mobile stage. Unlike traditional visual positioning methods which are prone to the effects of lighting and obstructions, and laser positioning methods that rely on environmental contours, a landmark recognition method is proposed based on the reflection intensities and shapes of the landmarks. This method combines triangulation matching algorithms with the least squares method to achieve precise initial positioning of

the mobile stage. Additionally, the system incorporates a distributed fusion Kalman filtering algorithm that integrates odometer data with laser data, further improving real-time positioning accuracy. By using artificial landmarks covered with 3M reflective film, the system effectively increases the laser detection range and enhances the accuracy of landmark recognition, making it particularly suitable for environments with unclear contours. The system has been implemented in an actual mobile stage, and test results indicate that the laser positioning system can achieve high positioning accuracy in both stationary and moving scenarios, and is resistant to changes in lighting conditions, performing exceptionally well even in real performance environments where lighting conditions vary dramatically.

The remainder of the paper is organized as follows. Section 1 introduces the hardware design of the mobile stage positioning system. Section 2 focuses on the design of the embedded software and the human-machine interface of the mobile stage. Section 3 is devoted to the design of the road signs detection algorithm, the initialization positioning algorithm and the positioning algorithm of a mobile stage. The experiments are presented in Section 4 and the conclusions are finally given in Section 5.

1 The hardware design of mobile stage positioning system

Based on the design requirements of the mobile stage positioning system, the system structure is illustrated in Fig. 1. This system comprises two primary components: the mobile stage and the artificial landmarks. The mobile stage utilizes these landmarks to determine its position relative to its own local coordinate system, allowing for precise calculation of its position and orientation. Fig. 1 offers a detailed overview of the mobile stage location system, highlighting the seamless integration of its critical components. The two-dimensional laser radar functions as the environmental sensor, gathering essential spatial data to identify landmarks. An embedded control board, powered by an i.MX 6Quad processor, processes sensor data and manages the motion unit. The motion unit, which includes servo drivers and omni-directional wheels, executes movement commands, enabling the stage to navigate smoothly and accurately. The hardware structure of the mobile stage is shown in Fig. 2. It is mainly composed of a two-dimensional laser radar, an embedded control board, a wireless router, and a motion control unit. The laser radar is used to scan the surrounding environment and collect the surrounding environ-

ment features. The embedded control board processes the laser data and sends motion control commands to the motor driver. In addition, the embedded control board is connected with a human-machine interface through the WiFi network.

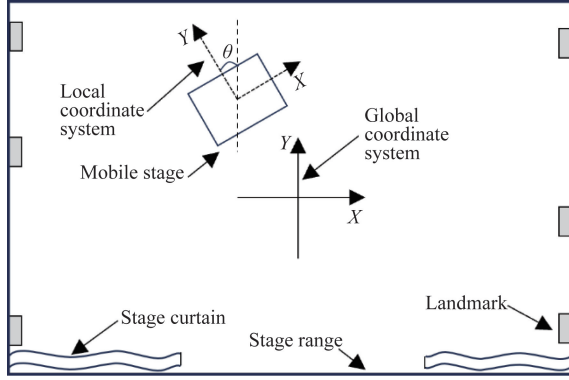


Fig. 1 The overall system structure

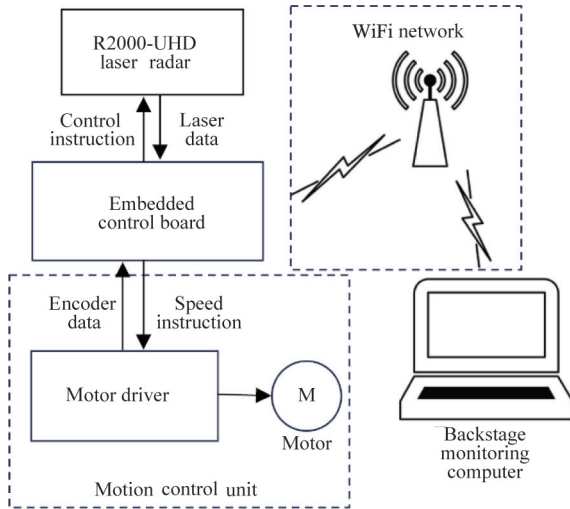


Fig. 2 Mobile stage hardware setup

1.1 2D laser radar

An R2000-UHD 2D laser radar from Pepperl + Fuchs is used in this paper. The laser radar has a minimum angular resolution of 0.014° , a maximum scanning frequency of 50 Hz, an effective measurement distance of 60 m (with reflection film), and is able to provide the angles, the distances, and the reflection intensity values. The communication of the laser radar is based on the hypertext transfer protocol (HTTP) and the transmission control protocol/Internet protocol (TCP/IP). In practical applications, the contours of the stage are not obvious, and the environment-based positioning method suffers from the occlusion induced by multiple mobile stages, which has a negative impact on the positioning accuracy. Therefore, the positioning

method based on artificial landmarks is used to locate the mobile stage. The reflection film is covered on the landmarks to increase the laser detection distance and achieves higher landmark identification accuracy.

1.2 Embedded controller

The embedded control board adopts an i. MX 6Quad processor based on the 64-bit ARM Cortex-A9 architecture from NXP semiconductors. Its highest frequency is up to 1.0 GHz and its memory is 1 GB, and its performance meets the processing requirements of laser data and the motion control. A Linux operating system operates on the processor.

1.3 Motion control unit

The motion control unit is mainly composed of the servo drivers, the motors, and the omnidirectional wheels. In order to drive the stage to achieve omnidirectional motions, a four-wheels structure is used in this paper, which is shown in Fig. 3, where X - Y represents the X - Y axis of the local stage coordinate system. The X_0 direction points to the front of the mobile stage, and v_1, v_2, v_3, v_4 represent the linear velocities of the four wheels, respectively. This structure enables the mobile stage to realize complex motions during the performance.

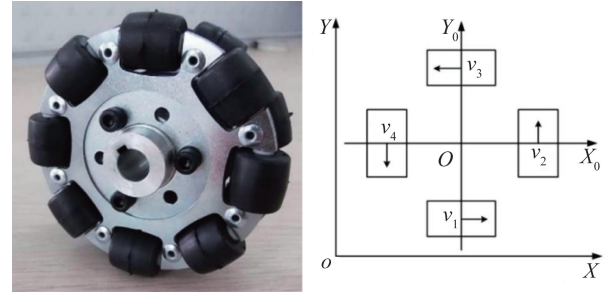


Fig. 3 Omnidirectional wheel and its coordinates

According to the four-wheels structure, the kinematic model of the stage is given by

$$\begin{bmatrix} v_1 \\ v_2 \\ v_3 \\ v_4 \end{bmatrix} = \begin{bmatrix} -\sin(90^\circ - \theta) - \frac{\cos(90^\circ - \theta)L}{2} \\ -\sin(90^\circ + \theta) - \frac{\cos(90^\circ + \theta)L}{2} \\ -\sin(90^\circ - \theta) - \frac{\cos(90^\circ - \theta)L}{2} \\ -\sin(90^\circ + \theta) - \frac{\cos(90^\circ + \theta)L}{2} \end{bmatrix} \begin{bmatrix} \dot{x} \\ \dot{y} \\ \dot{\theta} \end{bmatrix} \quad (1)$$

where, $[v_1 v_2 v_3 v_4]^T$ is the linear velocities of the four wheels, and $[\dot{x} \dot{y} \dot{\theta}]^T$ is the linear and the angular velocities of the moving stage in the global coordinate system, L represents the distance from the wheel to the

center of the mobile stage.

2 System software design

The positioning system software consists of the embedded software and the computer monitoring software, i. e. the human-machine interface. The embedded software processes the laser data in real time and controls the motion of the mobile stage. The computer monitoring software receives the mobile stage running status data in real time and sends control signals to the embedded software.

2.1 Embedded software design

The embedded software is implemented in C++ and runs on a Linux system. The control commands are sent to the laser radar through HTTP and TCP/IP is used to transfer the laser radar data. After receiving a frame of laser radar data, the software identifies the landmarks from the laser radar data, and calculates the pose of the mobile stage using the designed positioning algorithm. Based on the identification and positioning results, the embedded software controls the motor to execute corresponding control commands, and sends the stage pose to the monitoring software through the WiFi network. The flow chart of the embedded software operation is shown in Fig. 4.

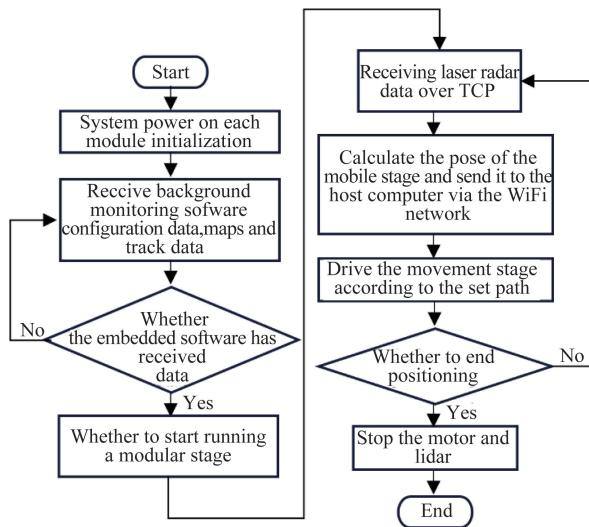


Fig. 4 Embedded software operation flow chart

2.2 Human-machine interface design

The human-machine interface is implemented in C# to realize positioning system parameters setting, real-time monitoring of motion status and data storage. The software interface is mainly composed of four functional blocks: real-time position display area, param-

eter setting area, button area, and coordinate display area. The real-time display area uses OpenGL to display the stage pose. The parameters of the laser radar and the type of landmarks can be set in the parameter setting area. The coordinate display area shows the coordinate of each landmark in the map and the pose of the mobile stage. The interface of the monitoring software is shown in Fig. 5.

The operation flow chart of the monitoring software is shown in Fig. 6. First, the monitoring software imports the extensible markup language (XML)-formatted map file and the track file, and sets the parameters of the mobile stage and the laser radar. Whereafter, the software connects the mobile stage and sends the positioning instruction to the stage, and starts the operation of the mobile stage. The mobile stage moves according to the set trajectory and uploads the pose data to the monitoring software in real time. The monitoring software stores the pose data in the database.

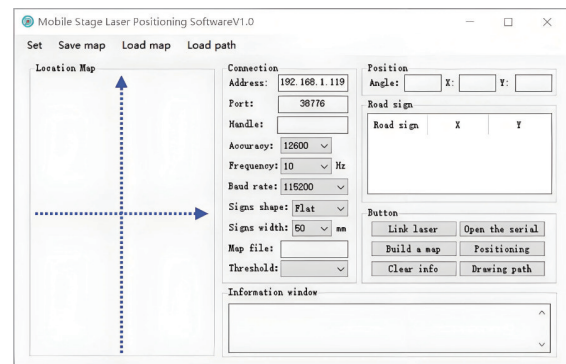


Fig. 5 Software interface

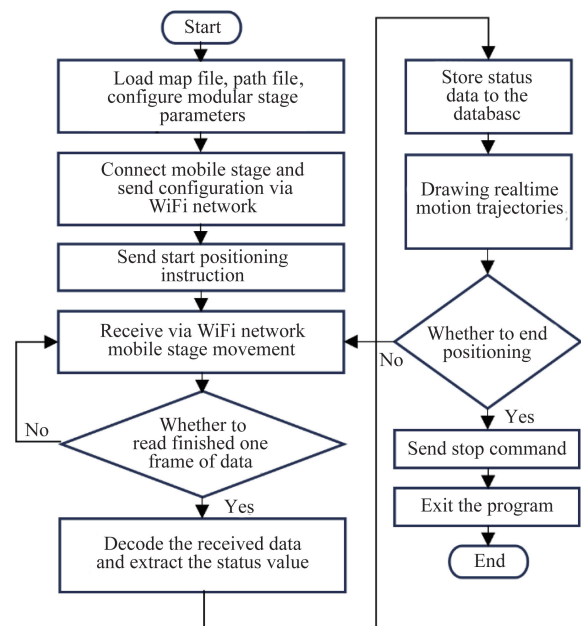


Fig. 6 Monitoring software operation flow chart

3 Positioning algorithms

The mobile stage positioning algorithm consists of three parts: a landmark extraction and identification algorithm, an initial positioning algorithm and a real-time positioning algorithm. The landmark extraction and identification algorithm extracts the landmarks from the environment and recognizes them. The initial pose of the mobile stage is calculated by the initial positioning algorithm. The real-time positioning algorithm achieves real-time positioning of the mobile stage.

3.1 Landmark extraction and identification algorithm

The landmark extraction and identification algorithm is the basis of the mobile stage positioning algorithm and provides accurate landmark coordinates data for subsequent algorithms.

The two-dimensional laser radar scans the surrounding environment to obtain the distance between the object and the laser radar, and collects the angle value and the reflection intensity^[21]. In order to enable the laser radar to effectively identify the landmarks in the environment, the 3M reflection film is covered on the artificial landmarks to improve the reflection intensity of the landmarks, thereby the reflection intensity of the landmark is significantly higher than the environmental reflection intensity, which is conducive to the extraction of landmarks^[22]. In the real environment, the metal surface may be recognized as a landmark because the reflection intensity of the metal surface is close to that of the landmark. Therefore, the width of the landmark needs to be detected after the landmark is identified. The landmark extraction and identification procedure is shown in Fig. 7.

The reflection intensity of the same material decreases with increasing distance. The reflection intensity of distant markers may be weaker than that of nearby markers. Therefore, a distance-related filter is proposed in this paper to screen out the landmarks from different distances. The reflection intensities are illustrated in Fig. 8.

The filter is designed as an inverse proportional function and is given as

$$f(d) = \frac{k_a}{k_b + d} - k_c \quad (2)$$

where, d represents the distance value detected by the laser radar; $f(d)$ is the threshold for reflection intensity corresponding to this distance. The hyperparameters k_a , k_b and k_c are critical to the system's performance

and must be carefully set. These hyperparameters are selected based on two primary factors: the system's operational range and the required sensitivity for accurate landmark detection. Typically, the values of k_a , k_b and k_c are determined through a precise calibration process. This process aims to balance detection accuracy with the specific environmental conditions present in the deployment area.

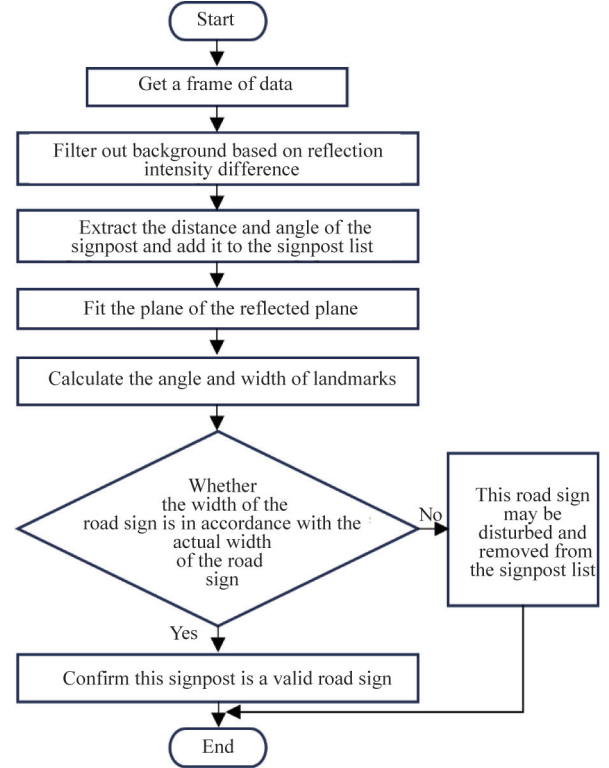


Fig. 7 The landmark extraction and identification flow chart

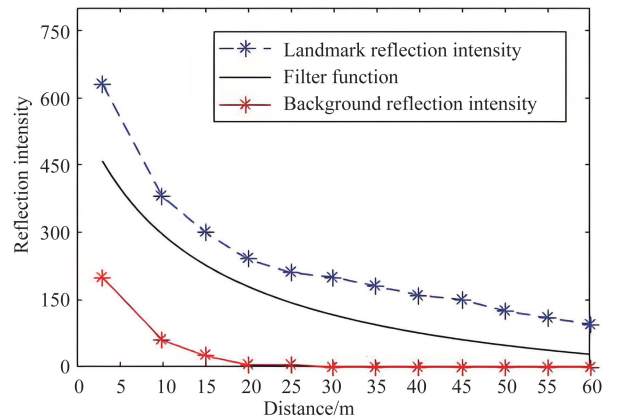


Fig. 8 Reflection intensity measured data and filter

There are materials with high reflection intensity in the natural environment, it is easy to cause misjudgment since the landmarks are recognized only depending on the reflection intensity. Therefore, the width of

the extracted landmark needs to be detected, which is shown in Fig. 9. First, the least squares method is used to obtain the angle α of the landmark surface in the laser radar coordinate system. The width of the landmark is calculated by

$$Width_{cal} \approx \frac{\Delta\varphi \cdot r}{\sin(\varphi - \alpha)} \quad (3)$$

where $\Delta\varphi$ is the angle difference between the two sides of the landmark; r and φ are the polar coordinates of the center of the landmark with respect to the local coordinate system, which are provided by the laser radar; $Width_{cal}$ is the estimated width of the landmark. Eq. (3) provides an estimation of the landmark's width using the angular difference $\Delta\varphi$ and the radial distance r , with φ indicating the landmark's angular position. Although it is theoretically possible to calculate the width of the landmark directly from the coordinates of the two sides of the landmark, it is easy to generate large errors in actual experiments. The error is due to the fact that the laser spot has a certain diameter, a part of the spot is illuminated on the landmark and the other part is illuminated on the background wall. Therefore, a strong reflection intensity may correspond to a background wall. The calculated width may differ from the actual landmark width, where the landmark may be mistaken as an interference.

Therefore, the landmark is detected based on the error between the measured landmark width and the actual width and the detected landmark is recognized as an effective landmark when the error is less than a given threshold. The error judgment criterion is given by

$$\frac{|Width_{cal} - Width_r|}{Width_r} < \lambda \cdot m(r) \quad (4)$$

where, $Width_r$ represents the actual width of the landmark, and the hyperparameter λ defines the acceptable error margin for detecting the landmark's width. The distance-related error coefficient $m(r)$ adjusts the allowable error based on the distance r from the radar, accommodating for greater measurement uncertainty at longer distances. These parameters are usually determined through experimental optimization to ensure reliable landmark identification under the specific conditions of the deployment environment.

3.2 Initial positioning algorithm

The initial positioning algorithm based on similar triangles matching is designed to get the initial pose of the mobile stage. The algorithm mainly consists of two steps: the landmark matching and the pose estimation. The landmark matching is to match the detected landmarks with the corresponding landmarks in the map. First, the center of the main stage is used as the coordinate origin, and the positive X -axis direction of the

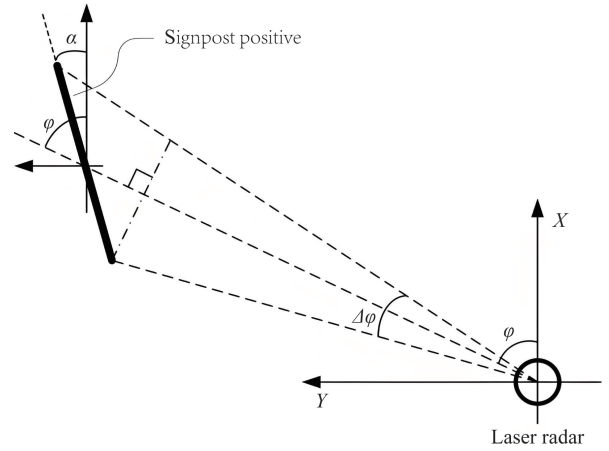


Fig. 9 Width detection schematic picture

global coordinate system coincides with the audience's direction. An appropriate number of landmarks are placed around the stage. The coordinates of the landmarks in the global coordinate system are denoted as $GF = \{F_{G_i}(x_{G_i}, y_{G_i}) \mid i = 1, 2, \dots, n\}$. The two-dimensional laser radar scans the surrounding environment. The laser radar center is used as the local coordinate origin, and the initial laser radar direction is used to establish the positive X -axis direction of the local coordinate system. The coordinates of the landmarks detected by laser radar in the local coordinate system are defined as $LF = \{F_{L_i}(x_{L_i}, y_{L_i}) \mid i = 1, 2, \dots, n\}$. The basic idea of the similar triangles matching algorithm is that when the two triangles which are respectively composed of three different detected landmarks in the sets GF and LF are approximately similar, three pairs of matching landmarks can be determined.

The pose estimation is to compute the pose of the local coordinate system with respect to the global coordinate system by using the matched triangles, that is, the pose of the mobile stage in the global coordinate system. Multiple matching problems may arise during the matching procedure. Therefore, it is necessary to check the pose and discard the wrong results. The initial positioning algorithm is summarized in the following algorithm.

Algorithm 1 Initial positioning algorithm based on similar triangles matching.

Step 1 Combine the landmarks in the sets GF and LF to obtain a set of triangles $GF = \{(A, B, C) \mid A, B, C \in GF\}$ and $LF = \{(A, B, C) \mid A, B, C \in LF\}$.

Step 2 Check the triangle vertices storage order. When the equality of triangle sides are used to judge the similar triangles, the mirrored two triangles may also satisfy this condition. Therefore, before the triangles are judged to be similar, the order of the three vertices

of the triangles needs to be checked to exclude the mirrored triangles. Denote the coordinates of the three vertices of the triangle as $A = (x_1, y_1)$, $B = (x_2, y_2)$, $C = (x_3, y_3)$. The necessary and sufficient condition for the three vertices being arranged counterclockwise is to satisfy the following inequality.

$$\begin{vmatrix} x_2 - x_1 & y_2 - y_1 \\ x_3 - x_1 & y_3 - y_1 \end{vmatrix} > 0 \quad (5)$$

Step 3 Find all the similar triangles in the two triangle sets. Compare the side lengths of all triangles in the two sets in turn to obtain all similar triangles. Each pair of matched triangles consists of three pairs of matched landmarks.

Step 4 Calculate all possible mobile stage poses. The coordinates of the corresponding landmarks in each pair of matched triangles are substituted into the least squares pose calculation formula to obtain the pose of the mobile stage in the global coordinate system. Each pair of matched triangles can be used to obtain a set of mobile stage pose. The least squares position calculation formula is given by

$$\underbrace{\begin{bmatrix} x_{L1} & y_{L1} & 1 & 0 \\ y_{L1} & x_{L1} & 0 & 1 \\ \vdots & \vdots & \vdots & \vdots \\ \vdots & \vdots & \vdots & \vdots \\ x_{Ln} & y_{Ln} & 1 & 0 \\ y_{Ln} & x_{Ln} & 0 & 1 \end{bmatrix}}_A \underbrace{\begin{bmatrix} \cos\theta \\ \sin\theta \\ x \\ y \end{bmatrix}}_H = \underbrace{\begin{bmatrix} x_{G1} \\ y_{G1} \\ \vdots \\ \vdots \\ x_{Gn} \\ y_{Gn} \end{bmatrix}}_b \quad (6)$$

Among them, the components in the matrix A are the landmark coordinates in the local coordinate system, and the vector b is composed of the corresponding landmark coordinates in the global coordinate system. The matrix H represents the pose matrix and is obtained by solving the above formula using the least square method.

Step 5 Delete the incorrect matched triangles and select the correct stage pose. It is easy to generate a mistake matching by simply using the equality of three sides as a judgment criterion. For example, a triangle in the set LT may be matched with several triangles in the set GT . There may be partially incorrect poses in all the possible poses calculated in Step 4. Therefore, using the acquired poses, the coordinates of the landmarks in the local coordinate system are converted into the global coordinate system. The transformed coordinates are compared with the coordinates of the landmarks in the map, and the number of correct matched landmarks and the average error are calculated. The pose with the most matched landmarks and the smallest average error is the correct pose.

Step 6 Calculate the optimal initial pose. Ac-

ording to the correct pose obtained in Step 5, the matching relationship between the laser-scanned landmarks and the landmarks in the map is obtained, and the coordinates of all the correct matched landmarks are substituted into the least squares pose calculation Eq. (6) to obtain the optimal initial pose $X(0)$ of the mobile stage.

The proposed pose calculation algorithm based on the least squares method is more accurate than the trilateration positioning method. The method can use more than three pairs of landmark coordinates to perform pose calculations to minimize the sum of squared errors.

3.3 Mobile stage positioning algorithm

The mobile stage positioning algorithm estimates the pose of the mobile stage in real time during the movement of the stage. Although the positioning algorithm based on a single laser radar is easy to implement and does not depend on the kinematics model, there are errors in the estimated pose, which may affect the matching of landmarks in the following and lead to poor positioning stability. Therefore, a distributed fusion Kalman filtering algorithm is designed to fuse landmarks information and odometer information to achieve higher positioning accuracy of the mobile stage. The odometer information is applied to obtain the predicted pose and the landmarks information is used in the measurement update procedure. Multiple landmarks information are implemented in a distributed way.

Denote the state vector in the global coordinate system of the mobile stage at time k as $X(k) = [x(k) \ y(k) \ \theta(k)]^T$. Using the estimated pose at the previous moment and the output of the odometer, the predicted $\hat{X}(k|k-1)$ in the global coordinate system at time k of the mobile stage can be obtained, that is

$$\hat{X}(k|k-1) = \hat{X}(k-1|k-1) + \begin{pmatrix} \Delta x(k) \\ \Delta y(k) \\ \Delta \theta(k) \end{pmatrix} \quad (7)$$

where $[\Delta x(k) \ \Delta y(k) \ \Delta \theta(k)]^T$ is the output of the odometer.

According to the predicted pose and coordinate conversion formula of the plane rectangular coordinate system, the predicted coordinates of the scanned landmark in the global coordinate system are obtained, and the coordinate conversion is calculated as

$$\begin{bmatrix} x_{Ei}(k) \\ y_{Ei}(k) \end{bmatrix} = \begin{bmatrix} \cos \hat{\theta}(k) & \sin \hat{\theta}(k) \\ -\sin \hat{\theta}(k) & \cos \hat{\theta}(k) \end{bmatrix} \begin{bmatrix} x_{Li}(k) \\ y_{Li}(k) \end{bmatrix} + \begin{bmatrix} \hat{x}(k) \\ \hat{y}(k) \end{bmatrix} \quad (8)$$

where, $[x_{Li} \ y_{Li}]^T$ is the coordinates of the scanned i th landmark in the local coordinate system; $[x_{Ei}(k)$

$y_{Ei}(k)]^T$ is predicted coordinates of the scanned landmark in the global coordinate system; $[\hat{x}(k) \hat{y}(k)]^T$ is the predicted position of the mobile stage in the global coordinate system; and $\hat{\theta}(k)$ is the predicted angle of the mobile stage in the global coordinate system.

Match the predicted coordinates of the scanned landmarks in the global coordinate system with the landmark coordinates stored in the map^[23]. When the distance difference between the two positions is less than a setting threshold, the matching is successful. Since the landmarks are scanned in turn, the landmarks information are received separately. Therefore, a distributed fusion strategy is applied to address the landmarks information sequence.

The observation vector $\mathbf{Z}_i(k) = [r_i(k) \varphi_i(k)]^T$ of the landmark is given by

$$\begin{bmatrix} r_i(k) \\ \varphi_i(k) \end{bmatrix} = \begin{bmatrix} \sqrt{\Delta x_i(k)^2 + \Delta y_i(k)^2} \\ \tan^{-1} \frac{\Delta y_i(k)}{\Delta x_i(k)} - \theta(k) + \frac{\pi}{2} \end{bmatrix} + \begin{bmatrix} v_1(k) \\ v_2(k) \end{bmatrix} \quad (9)$$

where $[r_i(k) \varphi_i(k)]^T$ is the polar coordinates the i th landmark, $\Delta x_i(k) = x(k) - x_{Gi}$, $\Delta y_i(k) = y(k) - y_{Gi}$. $[x_{Gi} \ y_{Gi}]^T$ is the coordinates of the artificial landmarks in the global coordinate system. The distributed fusion Kalman filtering algorithm for the mobile stage positioning is presented in Algorithm 2.

Algorithm 2 Distributed fusion Kalman filtering algorithm for mobile stage positioning

Step 1 The innovation is calculated as

$$\varepsilon_i(k) = \mathbf{Z}_i(k) - \hat{\mathbf{Z}}_i(k) \quad (10)$$

The innovation $\varepsilon_i(k)$ is the difference between the actual observation $\mathbf{Z}_i(k)$ and the predicted observation $\hat{\mathbf{Z}}_i(k)$. This residual quantifies the discrepancy between the observed and predicted positions of the landmarks.

Step 2 The variance of the innovation is given by

$$S_i(k) = \nabla \mathbf{H}(k-1)P(k|k-1)\nabla \mathbf{H}^T(k) + R_i(k) \quad (11)$$

The innovation variance $S_i(k)$ is calculated by combining the predicted state covariance $P(k|k-1)$ and the measurement noise covariance $R_i(k)$. This is linearized using the Jacobian matrix $\nabla \mathbf{H}(k)$ of the observation model to measure the uncertainty in the innovation.

Step 3 The Kalman gain is determined as

$$K_i(k) = P(k|k-1)\nabla \mathbf{H}^T(k)S_i^{-1}(k) \quad (12)$$

The Kalman gain $K_i(k)$ is obtained from the predicted state covariance $P(k|k-1)$, the transpose of the Jacobian $\nabla \mathbf{H}^T(k)$, and the inverse of the innovation covariance $S_i^{-1}(k)$. This gain adjusts the impact

of the innovation on the state estimate update.

Repeat Steps 1 – 3 for $i = 1, 2, \dots, m$; where m is the number of matched landmarks.

Step 4 The estimated are calculated as

$$\hat{X}(k|k) = \hat{X}(k|k-1) + \frac{1}{m} \sum_i (K_i(k)\varepsilon_i(k)) \quad (13)$$

The state estimate $\hat{X}(k|k)$ is refined by averaging the weighted innovations across all matched landmarks using their respective Kalman gains.

Step 5 The estimated state covariance is given by

$$P(k|k) = \left(\mathbf{I} - \frac{1}{m} \sum_i K_i(k)\nabla \mathbf{H}(k) \right) P(k|k-1) \quad (14)$$

The state covariance $P(k|k)$ is updated to reflect the new state estimate, thereby reducing overall uncertainty. This incorporates the Kalman gain and the linearized observation model.

In the presented mobile stage location system, the computational complexity primarily hinges on the landmark identification, the triangulation matching for initial positioning, and the distributed fusion Kalman filtering for real-time updates. The landmark identification process involves scanning the environment with a two-dimensional laser radar and matching detected points with predefined landmarks. The complexity of this step can be approximated as $O(N \log N)$ due to the need for sorting and searching within the set of N detected points. The initial positioning algorithm based on similar triangles matching involves comparing multiple sets of three landmarks to find the best match. The complexity here is dependent on the number of landmarks, with a potential complexity of $O(n^3)$ for matching, where n is the number of landmarks considered in the map. The Kalman filter's computational complexity is generally $O(m^3)$ for each update, where M is the size of the state vector. However, in the distributed fusion approach, this complexity is amortized over m landmarks, leading to an overall complexity of $O(m \cdot M^3)$ for the entire update process.

4 Experiments and analysis

Seven landmarks are implemented in the experiments, and the precise position of each landmark in the global coordinate system is evaluated and stored in the software system. A practical mobile stage for the experiment is designed as shown in Fig. 10, which is 1 m long and 1 m wide. In the experiment, the velocity of the mobile stage is kept between $0.4 \text{ m} \cdot \text{s}^{-1}$ and $0.6 \text{ m} \cdot \text{s}^{-1}$. The laser radar is placed at the front of

the mobile stage. The scanning frequency is set to be 10 Hz. Each detection frame contains 25 200 measurement points. The scanning range is $0^\circ - 180^\circ$. A 50.0 mm wide reflective landmark covered with 3M reflective film is used in the experiment. The landmark can be effectively recognized by the laser radar within a distance of 60 m. During the experiment, the OptiTrack 3D motion capture system is used to capture the reference pose of the mobile stage, and the algorithm is developed by applying the pseudocode in Algorithm 3. The OptiTrack system can provide the positioning precision of 0.1 mm at a 120 Hz sampling rate.

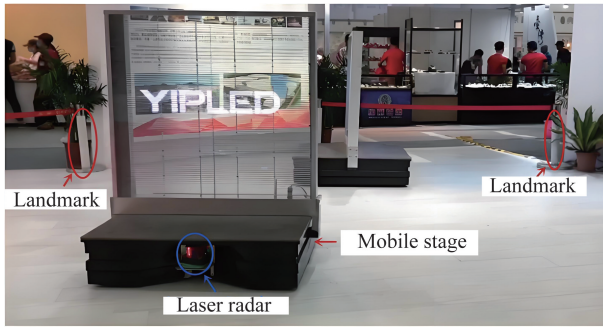


Fig. 10 The designed mobile stage in application

Algorithm 3 Pseudocode for mobile stage positioning algorithm

Inputs:

L – Set of landmark positions in the global coordinate system
 O – Odometry data stream from the mobile stage's motion control unit

Outputs:

X – Position and orientation of the mobile stage in the global coordinate system

```

1: Initialize  $X(0)$ ,  $P(0)$  // Initial state estimate and covariance
   // Part 1: landmark extraction and identification algorithm
2: for each time step  $k$  do
3:   Scan environment with laser radar
4:   Apply reflection intensity filter  $f(d)$  to extract landmarks
5:   Compute landmark width  $Width\_cal$ 
6:   Validate landmark with width error criterion
   // Part 2: initial positioning algorithm
7:   if  $k=0$  then
8:     for each set of detected landmarks  $j$  in  $M$  do
9:       Match landmarks using similar triangles method
10:      Compute pose of mobile stage using least squares method
11:      Select correct pose based on landmark matching validation
12:    $X(0) \leftarrow$  Optimal initial pose of the mobile stage

```

```

   // Part 3: real-time positioning algorithm
13: else
14:   Predict state and covariance
      $X(k|k-1) = f(X(k-1))$ 
   // State prediction function
      $P(k|k-1) = F \times P(k-1|k-1) \times F' + Q$ 
   // Predicted covariance,  $F$  is the state transition matrix,  $Q$  is process noise
15:   for each landmark  $i$  in  $L$  do
16:     Perform landmark detection and extract features
17:     Calculate innovation and innovation covariance
18:     Compute Kalman gain  $K_i(k)$ 
19:     Update state estimate  $X(k|k)$  with landmark  $i$  observation
20:   end for
21:   Update state covariance  $P(k|k)$  using the aggregated Kalman gains
22: end if
23: end for
24: return  $X$  // The final estimated position and orientation of the mobile stage

```

By applying the designed filter, only the reflection intensity of the landmark is greater than 0 among the reflection intensity data collected by the laser radar. According to this feature, the landmarks from different distances can be recognized intuitively. As shown in Fig. 11, some artificial landmarks are placed at different locations in the corridor, and the laser radar is used to scan the corridor to obtain the reflection intensities at different locations. The filtering result is shown in Fig. 12. From right part to the left part of the figure, the distance gradually increases and the reflection intensity decreases. When the distance increases to a certain extent, the landmark reflection intensity is so weak that it is close to the wall reflection intensity which is collected at a close distance. After filtering, the reflection intensity of the wall is normalized to 0 regardless of the disturbance. Although the reflection intensity of the landmark is weakened after filtering, it is more obvious than the reflection intensity of the wall.

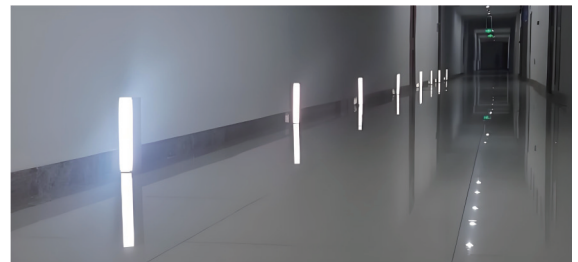


Fig. 11 Testing scenarios

Fig. 13 shows the comparison between the trajectory estimated by the proposed positioning method and

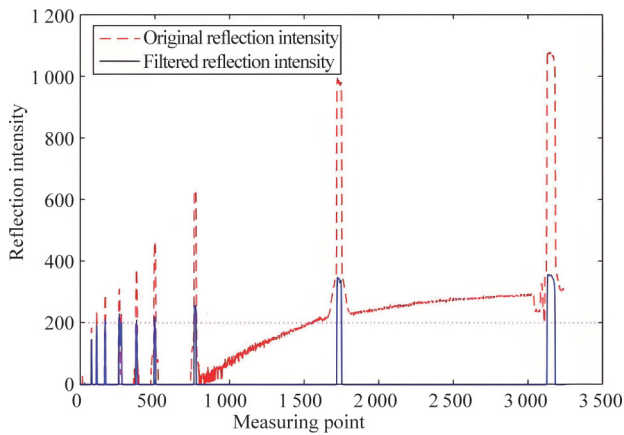


Fig. 12 Comparison of the original reflection intensity and the reflection intensity after filtering

the reference trajectory, and the estimated trajectory error is shown in Fig. 14. It can be seen from Figs. 13 and 14 that the estimated trajectory basically coincides with the reference trajectory, and the positioning precision is high where the maximum position error is within 20.0 mm and the average position error is 6.5 mm. It should be noted that there is an installation error between the real center position and the center position of the mobile stage captured by the OptiTrack system, and this installation error will always exist throughout the experiment. In some periods of time, the positioning error fluctuates dramatically, which indicates that there is still a lack of stability in the positioning system and remains to be solved. The comparison between the estimated angle and the true angle as well as the angle error are shown in Figs. 15 and 16, respectively. It can be seen from Figs. 15 and 16 that the proposed method provides satisfactory angle estimation accuracy of the mobile stage. The maximum angle error is within 1.26° and the average angle error is 0.28° . The results show that the proposed method manifests a high level of feasibility and positioning accuracy.

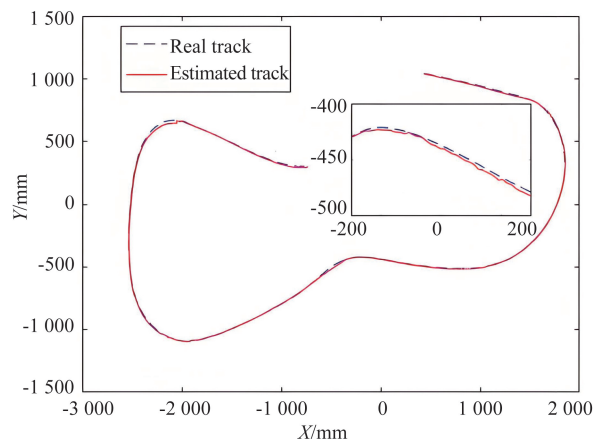


Fig. 13 Estimated trajectory and true trajectory

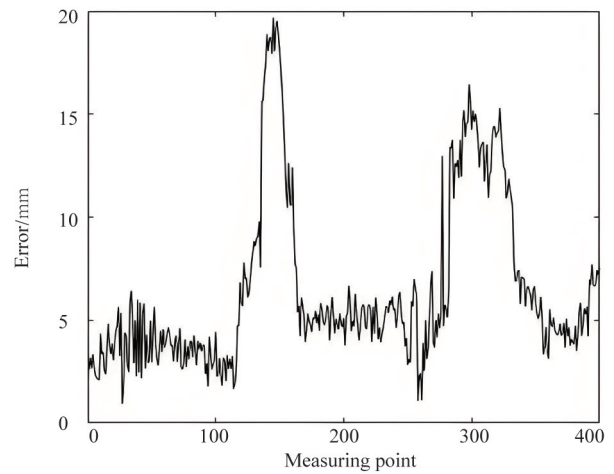


Fig. 14 Trajectory error

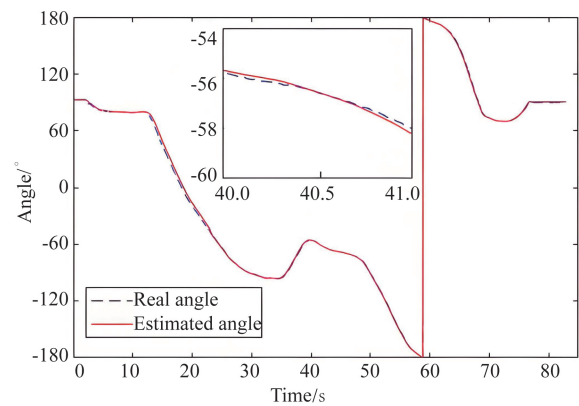


Fig. 15 Estimated angle and true angle

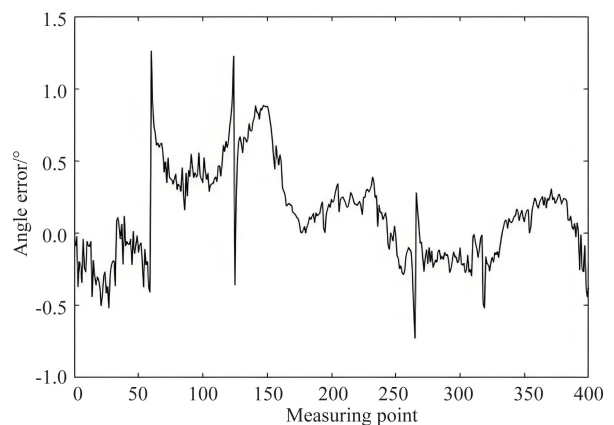


Fig. 16 Angle error

To demonstrate the feasibility and superiority of the proposed algorithm, it is compared with WiFi-based positioning and laser rader odometry based positioning. Fig. 17 shows the comparison experiment scene, and Fig. 18 shows the results of different algorithms in recovering the trajectory of an intelligent robot following the same motion path. As seen from the fig-

ure, the ‘Mobile stage positioning algorithm’ obtained by the proposed algorithm almost overlaps with the ‘Real track’, particularly in sections where the trajectory is more complex, indicating a higher level of accuracy. In contrast, the trajectories estimated by the other two methods show some deviation from the real trajectory, especially in areas with significant local path variations. In conclusion, the proposed method has high feasibility and can improve positioning accuracy.



Fig. 17 Comparative experimental scenario

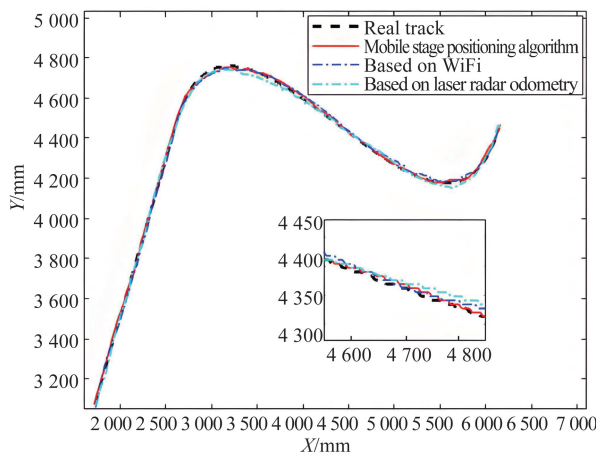


Fig. 18 Comparative experiment

5 Conclusions

This paper has designed a laser radar based mobile stage location system to achieve a high level of positioning accuracy. Its contributions lie in the following aspects.

(1) A novel landmark identification method is presented based on the landmark reflection intensities and shapes to address the complex background environment.

(2) A distributed fusion Kalman filtering algorithm is applied to fuse multiple landmarks information and the odometer information to achieve high positioning precision of the mobile stage, and the initial pose of the mobile stage is calculated by using the triangle matching algorithm and the least squares method.

(3) Both hardware and software are designed to achieve real-time control, positioning and monitoring of the mobile stage.

The proposed positioning method has been used in practical applications and the effectiveness of the sys-

tem has been evaluated through practical experiments. The results show that the proposed method manifests a high level of feasibility and positioning accuracy.

References

- [1] KULHANEK J, DERNER E, BABUSKA R. Visual navigation in real-world indoor environments using end-to-end deep reinforcement learning[J]. *IEEE Robotics and Automation Letters*, 2021, 6(3) : 4345-4352.
- [2] SJANIC Z, SKOGLUND M A, GUSTAFSSON F. EM-SLAM with inertial/visual applications[J]. *IEEE Transactions on Aerospace and Electronic Systems*, 2017, 53(1) : 273-285.
- [3] MINAEIAN S, LIU J, SON Y J. Vision-based target detection and localization via a team of cooperative UAV and UGVs[J]. *IEEE Transactions on Systems Man Cybernetics-Systems*, 2016, 46(7) :1005-1016.
- [4] RAFAEL M C, PARRA C, DEVY M. Visual navigation in natural environments: from range and color data to a landmark-based model[J]. *Autonomous Robots*, 2002, 13(2) :143-168.
- [5] JANG C, KIM Y K. Drift compensation of mono-visual odometry and vehicle localization using public road sign database[J]. *International Journal of Automotive Technology*, 2019, 20(6) :1245-1254.
- [6] CAZZORLA A, DE ANGELIS G, MOSCHITTA A, et al. A 5.6-GHz UWB position measurement system [J]. *IEEE Transactions on Instrumentation and Measurement*, 2013, 62(2) :675-683.
- [7] SUSKI W, BANERJEE S, HOOVER A. Using a map of measurement noise to improve UWB indoor position tracking[J]. *IEEE Transactions on Instrumentation and Measurement*, 2013, 62(8) : 2228-2236.
- [8] MÜLLER P, WYMEERSCH H, PICHÉ R. UWB positioning with generalized Gaussian mixture filters[J]. *IEEE Transactions on Mobile Computing*, 2014, 13(10) : 2406-2414.
- [9] DE ANGELIS G, MOSCHITTA A, CARBONE P. Positioning techniques in indoor environments based on stochastic modeling of UWB round-trip-time measurements[J]. *IEEE Transactions on Intelligent Transportation Systems*, 2016, 17(8) : 2272-2281.
- [10] ZHANG W, LIU N, ZHANG Y F. Learn to navigate maplessly with varied LiDAR configurations: a support point-based approach[J]. *IEEE Robotics and Automation Letters*, 2021, 6(2) : 1918-1925.
- [11] NISHIZAWA T, OHYA A, YUTA S. An implementation of on-board position estimation for a mobile robot-EKF based odometry and laser reflector landmarks detection [C]//1995 IEEE International Conference on Robotics and Automation. Nagoya, Japan: IEEE, 1995: 395-400.
- [12] VAZQUEZ-MARTIN R, NUÑEZ P, DEL TORO J C, et al. Adaptive observation covariance for EKFSLAM in indoor environments using laser data[C]//2006 IEEE Mediterranean Electrotechnical Conference. Benalmadena, Spain: IEEE, 2006: 445-448.
- [13] PENIZZOTTO F, SLAWINSKI E, MUT V. Laser radar based autonomous mobile robot guidance system for olive

- groves navigation[J]. IEEE Latin America Transactions, 2015, 13(5): 1303-1312.
- [14] ZOU Q, WANG X. A robot navigation method based on laser and 2D code[C]// 2016 IEEE International Conference on Information and Automation. Ningbo, China: IEEE, 2017: 485-490.
- [15] LIU M, HUANG S, DISSANAYAKE G. Feature based SLAM using laser sensor data with maximized information usage[C]// 2011 IEEE International Conference on Robotics and Automation. Shanghai, China: IEEE, 2011: 1811-1816.
- [16] NARAYANA K, GOULETTE F, STEUX B. Planar landmark detection using a specific arrangement of laser scanners[C]// IEEE/ION Position Location and Navigation System Conference. Indian Wells, USA: IEEE, 2010: 1057-1069.
- [17] RONZONI D, OLMI R, SECCHI C, et al. AGV global localization using indistinguishable artificial landmarks[C]// 2011 IEEE International Conference on Robotics and Automation. Shanghai, China: IEEE, 2011: 287-292.
- [18] STEPHEN L S, SCHWAGER M, RUS D. Persistent robotic tasks: monitoring and sweeping in changing environments[J]. IEEE Transactions on Robotics, 2011, 28(2): 410-426.
- [19] HU H S, GU D B. Landmark-based navigation of industrial mobile robots[J]. Industrial Robot, 2000, 27(6): 458-467.
- [20] LOEVSKY T, SHIMSHONI I. Reliable and efficient landmark-based localization for mobile robots[J]. Robotics and Autonomous Systems, 2010, 58(5): 520-528.
- [21] OLLIVIER E, PARENT M. Odometric navigation with matching of landscape features[C]// International Conference on Control, Automation, Robotics and Vision. Singapore: IEEE, 2002: 757-762.
- [22] GUIVANT J, NEBOT E, BAIKER S. High accuracy navigation using laser range sensors in outdoor applications [C]// IEEE International Conference on Robotics and Automation. San Francisco, USA: IEEE, 2000: 3817-3822.
- [23] BAILEY T. Mobile robot localisation and mapping in extensive outdoor environment[D]. Sydney: University of Sydney, 2002.

WANG Bo, born in 1982. He received his Ph. D degree in College of Information Engineering of Zhejiang University of Technology in 2009. His research interests include electronic technique and automatic control systems.